Generation of cross-polarized photon pairs in a microstructure fiber with frequency-conjugate laser pump pulses

J. Fan and A. Migdall

Optical Technology Division
National Institute of Standards and Technology
100 Bureau Drive, Mail Stop 8441, Gaithersburg. MD 20899-8441
Jfan@nist.gov

Abstract: We propose and experimentally demonstrate the generation of cross-polarized photon pairs via four-wave mixing with cross-polarized frequency-conjugate laser pump pulses. This method can be used for various quantum information applications such as the preparation of Bell-states.

References and links

1. C. Kurtsiefer, P. Aarda, M. Halder, H. Weinfurter, P. M. Gorman, P. R. Tapster, "Quantum cryptography: A step towards global key distribution," Nature **419**, 450 (2002).
2. M. Aspelmeyer, H. R. Böhm, T. Gyatso, T. Jennewein, R. Kaltenbaek, M. Lindenthal, G. Molina Terriza, A. Poppe, K. Resch, M. Taraba, R. Ursin, P. Walther, and A. Zeilinger, "Long-distance free-Space distribution of quantum entanglement," Science **301**, 621 (2003).
3. I. Marcikic, H. de Riedmatten,W. Tittel, H. Zbinden, M. Legre, and N. Gisin, "Distribution of time-bin entangled qubits over 50 km of optical fiber," Phys. Rev. Lett. **93**, 180502 (2004).
4. D. C. Burnham, D. L. Weinberg, "Observation of simultaneity in parametric production of optical photon pairs," Phys. Rev. Lett. **25**, 84 (1970).
5. S. Friberg, C. K. Hong, and L. Mandel, "Measurement of time delays in the parametric production of photon pairs," Phys. Rev. Lett. **54**, 2011 (1985).
6. S. Friberg and L. Mandel, "Production of squeezed states by combination of parametric down-conversion and harmonic generation," Opt. Commun. **48**, 439 (1984).
7. P. G. Kwiat, E. Waks, A. G. White, I. Appelbaum, and P. H. Eberhard, "Ultrabright source of polarization-entangled photons," Phys. Rev. A**60**, R773 (1999).
8. C. Kurtsiefer, M. Oberparleiter, and H. Weinfurter, "High-efficiency entangled photon pair collection in type-II parametric fluorescence," Phys. Rev. A **64**, 023802 (2001)
9. E. Brannen, F. R. Hunt, R. H. Adlington, R. W., Hicholls, "Application of nuclear coincidence methods to atomic transitions in the wavelength range 2000-6000A," Nature **175**, 810 (1955).
10. A. Kuzmich, W. P. Bowen, A. D. Boozer, A. Boca, C. W. Chou, L.-M. Duan, and H.J. Kimble, "Generation of nonclassical photon pairs for scalable quantum communication with atomic ensembles," Nature **423**, 731 (2003).
11. C. Santori, D. Fattal, J. Vu, G. S. Solomon, Y. Yamamoto, "Indistinguishable photons from a single-photon device," Nature **419**, 594 (2002).
12. S. Tanzilli, F. D. Riedmatten, W. Tittle, H. Zbinden, P. Baldi, M. D., Micheli, D. B. Ostrowsky, N. Gisin, "Highly efficient photon-pair source using periodically poled lithium niobate waveguide," Electron. Lett. **37**, 26 (2001).
13. S. J. Mason, M. A. Albota, F. Konig, and F. N. C. Wong, "Efficient generation of tunable photon pairs at 0.8 and 1.6 μm," Opt. Lett. **27**, 2115 (2002).
14. F. Konig, E. J. Mason, F. N. C. Wong, and M. A. Albota, "Efficient spectrally bright source of polarization-entangled photons," Phys. Rev. A **71**, 033805 (2005).
15. T. A. Birks, J. C. Knight, and P. St. J. Russell, "Endlessly single-mode photonic crystal fibers," Opt. Lett. **22**, 961 (1997).
16. M. Fiorentino, P. L. Voss, J. E. Sharping, and P. Kumar, "All-fiber photon-pair source for quantum communication," IEEE Photonics Tech. Lett. **14**, 983 (2002).

17. A. Dogariu, J. Fan, and L.J. Wang, "Correlated photon generation for quantum cryptography," NEC R&D Journal **44**, 294 (2003).
18. J. E. Sharping, J. Chen, X. Li, P. Kumar, and R. S. Windeler, "Quantum-correlated twin photons from microstructure fiber," Opt. Express **12**, 3086-3094 (2004), http://www.opticsexpress.org/abstract.cfm?URI=OPEX-12-14-3086
19. J. G. Rarity, J. Fulconis, J. Duligall, W. J. Wadsworth, and P. S. J. Russell, "Photonic crystal fiber source of correlated photon pairs," Opt. Express **13**, 534-544 (2005), http://www.opticsexpress.org/abstract.cfm?URI=OPEX-13-2-534
20. J. Fan, A. Dogariu, L. J. Wang, "Generation of correlated photon pairs in a microstructure fiber," Opt. Lett. **30**, 1530 (2005).
21. G. P. Agrawal, *Nonlinear Fiber Optics*, 2nd ed. (Academic Press, 1995).
22. H. Takesue and K. Inoue, "Generation of polarization-entangled photon pairs and violation of Bell's inequality using spontaneous four-wave mixing in a fiber loop," Phys. Rev. A **70**, 031802(R) (2004).
23. X. Li, P. Voss, J. E. Sharping, P. Kumar, "Optical-fiber source of polarization-entangled photon pairs in the 1550 nm telecom band," Phys. Rev. Lett. **94**, 053601 (2005).
24. T. E. Kiess, Y. H. Shih, A. V. Sergienko, and C. O. Alley, "Einstein-Podolsky-Rosen-Bohm experiment using pairs of light quanta produced by type-II parametric down-conversion," Phys. Rev. lett. **71**, 3893 (1993).
25. L. J. Wang, C. K. Hong, and S. R. Friberg, "Generation of correlated photons via four-wave mixing in optial fibers," J. Opt. B: Quantum and Semiclass. Opt. **3**, 346 (2001).
26. P. L. Voss and P. Kumar, "Raman-effect induced noise limits on $\chi^{(3)}$ parametric amplifiers and wavelength converters," J. Opt. B: Quantum and Semiclass. Opt. **6**, 762 (2004).

1. Introduction

Correlated photons have been used to study quantum information science, especially in the areas of quantum communication and cryptography [1-3]. In most experiments, correlated photons were generated through parametric down conversion (PDC) of an ultraviolet (UV) beam in a bulk nonlinear crystal. This photon pair generation method was first demonstrated more than three decades ago and has been studied ever since [4-8]. In addition to this method, there are other approaches to generate correlated photons. They include two-photon emission from atoms [9, 10], quantum dots [11], as well as PDC in engineered crystals such as Periodically Poled Lithium Niobate (PPLN) [12-14], which exhibit higher conversion efficiencies than bulk crystals.

It is of great interest to directly generate correlated photons in fibers. Being part of an optical communication network, correlated photons generated in fibers can be 100 % collected and delivered to realize quantum cryptography applications. Compared to conventional fibers, microstructure fiber (MF) has a very large refractive-index contrast between its silica core and its surroundings patterned with air holes, allowing for a very small core size and mode field diameter. This, along with the fact that fiber allows very long interaction lengths, results in high effective optical nonlinearity in a MF with much lower optical pump power [15]. Also, the MF can be engineered to meet a range of specific applications and pump wavelengths. Overall, this ease of collection, low pump power, and convenient pump wavelength selection makes MF an excellent candidate source to provide correlated photons.

It has been demonstrated that by injecting a laser beam (ω_0) into a single mode optical fiber (SMF) or a MF, correlated Stokes (ω_s) and anti-Stokes (ω_{as}) photon pairs at conjugate frequencies are generated via degenerate four-wave mixing process (FWM) at the phase matching condition, $\omega_s + \omega_{as} = 2\omega_0$ [16-19]. In a reverse process, it was also shown that by recombining these pairs of parallel-polarized conjugate photons in a second fiber, photon pairs can be generated at the middle frequency with good efficiency, $2\omega_0 = \omega_s + \omega_{as}$ [20].

It is known that in an ideal single mode fiber (SMF), a mode excited with its polarization along principal axis *x* of the fiber does not couple to the mode with orthogonal *y*-polarization state [21]. This effect has been used to generate polarization-entangled photon pairs by synchronizing two orthogonal but degenerate FWM processes in a dispersion-shifted fiber (DSF) [22, 23]. Two same wavelength laser pulses with polarizations perpendicular to each other coupled into a DSF, each create a correlated photon pair in the polarization state of

|H$_s$H$_i$> or |V$_s$V$_i$>. |H> and |V> are two orthogonally polarized photon states and "s" and "i" stand for signal (anti-Stokes) and idler (Stokes) photons at different wavelengths. |H$_s$H$_i$> and |V$_s$V$_i$> are interferometrically combined. With proper phase and polarization control, each of the four Bell-states can be prepared. This method has also been used to interferometrically combine two separate PDC processes to prepare a bright polarization-entangled photon pair source using two bulk crystals [7, 8] or PPLNs [14].

These experiments generating correlated photons via FWM in fibers are based on χ_{xxxx} or χ_{yyyy}, which are components of the third order nonlinear susceptibility tensor $\chi^{(3)}$. Photon pairs generated in these processes are co-polarized with the pump laser beam. In this paper, we propose to generate cross-polarized correlated photons by make using of χ_{xyxy}, a different component of the susceptibility tensor $\chi^{(3)}$.

We overlap a Stokes ($E_s(t,z)$) laser pulse polarized along principal axis x with an anti-Stokes ($E_{as}(t,z)$) laser pulse polarized along principal axis y in a MF, generating correlated photon pairs by FWM at the middle frequency ω_0 in the state of $|x> |y>$ when phase matching condition is satisfied. Here $|x>$ and $|y>$ are polarization states along axes x and y, respectively. The optical field is tightly confined in the single spatial mode due to the big transverse refractive index gradient in the MF. The spatial wave function is dropped for simplicity without losing generality. The polarization mode dispersion (PMD) induced temporal distinguishability between the two photons in polarization states $|x>$ and $|y>$ can be compensated by passing the photons through birefringent optics such as another piece of MF with appropriate orientation and length. Then at the exit, the two photons are indistinguishable in space, time, and color. This is similar to the way of generating correlated photon pairs in a collinear type-II PDC process [24]. Thus, Bell-states can be prepared in the postselection scheme 50% of the time, which can be used for various quantum information applications. This scheme with a pair of orthogonally polarized pump pulses is shown in Fig. 1.
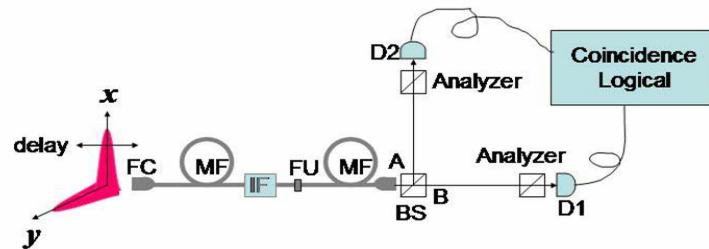

Fig. 1. Schematic experimental setup to test Bell's inequality. FC: fiber coupler, MF: microstructure fiber (first one used for generation of cross-polarized photon pairs, second one for phase compensation), BS: non-polarizing beam splitter, FU: fiber union, IF: interference filter at middle frequency, D1 and D2: photon detectors.

2. Experiments and discussion

Instead of an experiment such as testing Bell's inequality, for this current initial experiment our goal is to examine the generation of cross-polarized photon pairs by FWM with cross-polarized laser pump pulses in an optical fiber. The experimental setup is shown in Fig. 2. A 3 ps laser pulse is coupled into microstructure fiber MF1 with wavelength at 835 nm (the zero dispersion wavelength of microstructure fibers: MF1 and MF2 [17, 20]), driving quasi-continuum generation through FWM, self-phase modulation and other optical nonlinear mechanisms in MF1. The output from MF1 is collimated and directed onto a high resolution grating (2,200 grooves/mm). Using a two-pass grating configuration and two narrow slits, a pair of pulses at conjugate frequencies: Stokes (837 nm) and anti-Stokes (833 nm) are selected. The two-pass arrangement puts these two pulses in the same single spatial mode where they are coupled into a 1.5 m fiber, MF2. Polarizations of these two pulses are parallel to each other and oriented at 45° with respect to axes x and y.

After MF2, we insert a half-wave plate and a polarizing beam splitter (PBS) into the beam path to spatially separate photons of different polarizations. We then direct these two beams of different polarizations onto a second grating (2,200 grooves/mm). Again, using a two-pass grating configuration and two narrow slits, only those photons at the wavelength of 834.5 nm are selected and sent to photon counters. The collection bandwidth is determined to be 0.2 nm for each of the beam detection channel. Signals from the two photon counters are sent to a coincidence circuit. Half waveplates in the beam path are placed to maximize the yield of photons of interest.
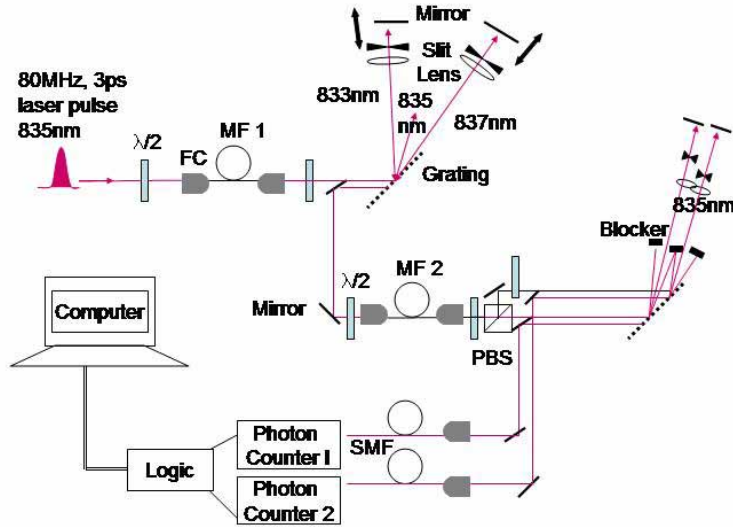

Fig. 2. Schematic experimental setup. PBS: polarizing beam splitter, SMF: single mode fiber, λ/2: half-wave plate. MF1 and MF2 are microstructure fibers.

With polarization oriented at 45° with respect to axes x and y, the Stokes (anti-Stokes) pulse is split into two pulses with equal power in MF2 polarized along axes x and y, respectively, resulting in a four-pulse co-propagation configuration in MF2. The electric field of the four-pulse is,

$$E_s(t,z)=E_{sx}(t,z)\mathbf{x}+E_{sy}(t,z)\mathbf{y}, \tag{1a}$$
$$E_{as}(t,z)=E_{asx}(t,z)\mathbf{x}+E_{asy}(t,z)\mathbf{y}. \tag{1b}$$

For this short fiber, group velocity dispersion (GVD) is negligible [17]. Pulses polarized along axis x walk off from pulses polarized along axis y in MF2 due to PMD. By adjusting the relative delay of the anti-Stokes pulse with respect to the Stokes pulse in MF2, we can arrange to overlap either $E_{sx}(t,z)\mathbf{x}$ with $E_{asy}(t,z)\mathbf{y}$ or $E_{sy}(t,z)\mathbf{x}$ with $E_{asx}(t,z)\mathbf{y}$. These delay configurations (Fig. 3(a)) are described below.

(1) At delay t_1, overlap only occurs between E_{asx} and E_{sy}. In this case we launch the anti-Stokes pulse ahead of the Stokes pulse into MF2. Cross-polarized photon pairs in the state $|x\rangle|y\rangle$ are generated by FWM at the middle frequency. This is similar to a collinear degenerate type-II PDC process [24].

(2) At delay t_3, overlap only occurs between E_{asy} and E_{sx}, generating cross-polarized photon pairs in the state $|x\rangle|y\rangle$ at the middle frequency through FWM. In this case, we launch the Stokes pulse ahead of the anti-Stokes pulse into MF2.

(3) At a delay t_2 between t_1 and t_3, both Stokes and anti-Stokes pulses enter MF2 at the same time. Before the PMD walk-off, FWM can occur in both parallel- and cross-polarization schemes. For FWM with parallel-polarized pump pulses, E_{asx} overlaps with E_{sx} to generate photon pairs in the polarization state $|x\rangle|x\rangle$ along axis x, E_{asy} overlaps with E_{sy} to generate photon pairs in the polarization state $|y\rangle|y\rangle$ along axis y. These two processes are coherent,

forming a superposed state $\frac{1}{\sqrt{2}}(|x\rangle|x\rangle+e^{i\phi}|y\rangle|y\rangle)$ with all photons generated at the middle frequency. This scheme has been used to generate polarization-entangled photon pairs in a DSF [22, 23]. Here ϕ is the relative phase due to PMD and the phase difference between the two pump pulses. In the meantime, FWM also occurs between the cross-polarized pump pulses. The overlaps of E_{asx} with E_{sy} and E_{asy} with E_{sx} generate correlated photons in the polarization state $|x\rangle|y\rangle$, although the generation rate is smaller by one order of magnitude than that of FWM with parallel-polarized pump pulses because $3\chi_{xyxy} \sim \chi_{xxxx}$ (χ_{yyyy}). After PMD walk-off, correlated photon pairs are only generated in the parallel polarization scheme as long as temporal coherence is retained between E_{asx} and E_{sx}, and E_{asy} and E_{sy}.

These three cases are illustrated in Fig. 3(a), in which the PMD walk-offs are exaggerated for better view. In Fig. 3(b), the contrast C/A, defined as the ratio between coincidence count rate and accidental coincidence count rate, is plotted as a function of the relative delay between the anti-Stokes and Stokes pulses. The filled dots and open dots were obtained from two separate measurements carried out with pump powers different by a ratio of 2, both exhibiting a three-peak pattern. Although the three coincidence peaks are not completely resolved from each other due to limited PMD walk-off in the short fiber, the three-peak pattern is evidence of the three cases discussed above. The coincidence peaks at delay t_1 and t_3 are mainly due to the cross-polarized correlated photons generated by FWM with cross-polarized pump pulses. The peak at t_2 is dominated by contribution from $\frac{1}{\sqrt{2}}(|x\rangle|x\rangle+e^{i\phi}|y\rangle|y\rangle)$ [23], generated from FWM with parallel-polarized pump pulses. The normalized spectra of the conjugate pump pulses used in the measurements are plotted in Fig. 3(c).

The measured contrast C/A in this cross-polarized pump scheme is lower than that (C/A ~ 8) of a similar experiment performed in the parallel-polarized scheme [20]. This is expected because while Raman scattering is same for both polarization schemes at the same amount of pump power, the gain of FWM with cross-polarized pump pulses is much smaller than the gain of FWM with parallel-polarized pump pulses because of $3\chi_{xyxy} \sim \chi_{xxxx}$. In the experiment, photon count rate at each detector is nearly linearly proportional to pump power, indicating that Raman scattering dominates. At delay time t_1, with an average pump power of 100 μW, (or a peak power of ~ 0.4 W, for a 3 ps pulse width and 80 MHz repetition rate), the photon count rate is ~ 24 kHz at detector 1 (with an overall detection efficiency of 0.08) and ~ 27 kHz at detector 2 (with an overall detection efficiency of 0.09). The observed photon coincidence rate is ~ 4 Hz (after subtraction of accidental and dark counts).

The phase-matching of FWM with parallel-polarized pump pulses in the MF has been examined [17, 20]. The phase-matching shows clear dependence on pump power when GVD is significant for well wavelength-separated Stokes and anti-Stokes photons [17]. When the wavelengths of Stokes and anti-Stokes photons are close to each other and pump power is low, the phase-matching condition is automatically satisfied [20]. This is the case of our experiment with the two pump pulses separated by 4 nm in wavelength and an average pump power of 100 μW. Because we are more concerned about generation of correlated photons with two cross-polarized laser pulses, we performed a phase-matching measurement at delay t_1, when the x-polarized anti-Stokes pulse E_{asx} optimally overlaps the y-polarized Stokes pulse E_{sy} in MF2. Fixing the wavelength of Stokes pulse, we saw the measured contrast C/A increase from the baseline (where C/A=1) to the peak and then decrease to the baseline again when varying the anti-Stokes pulse through the phase-matching wavelength, showing clear evidence of the phase-matching FWM process with cross-polarized pump pulses in MF2.

From the separations of coincidence peaks shown in Fig. 3(b), the mode birefringence of MF2 can be estimated to be $\Delta n \approx 1.6 \times 10^{-3}$.
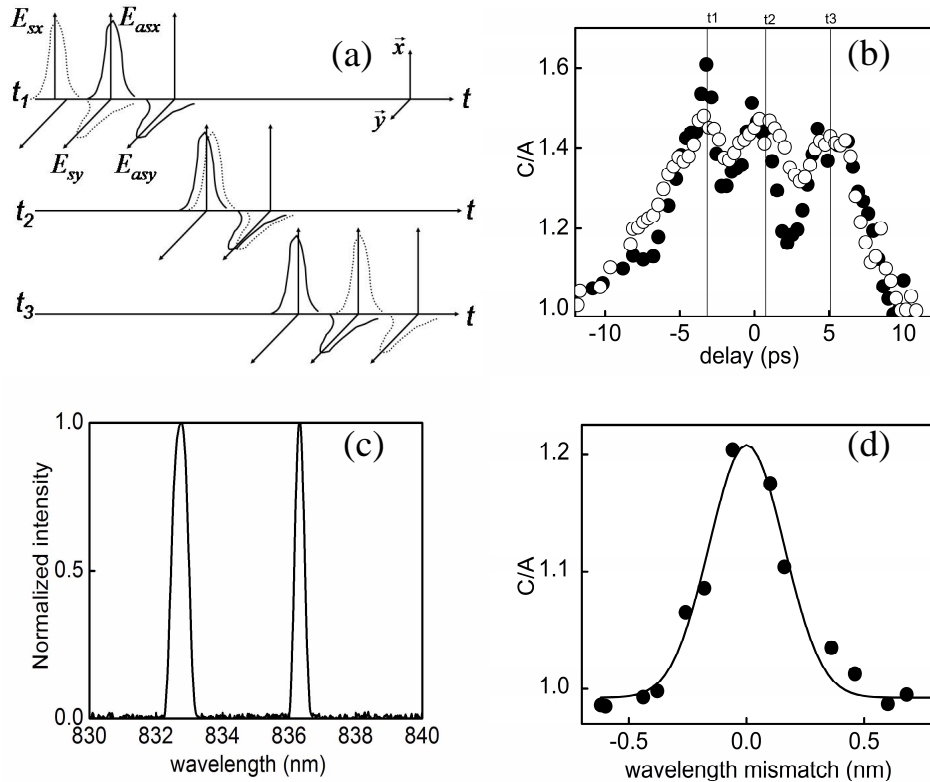
Fig. 3. (a) Three cases of two different schemes to generate correlated photons in MF2, with electric field components labeled. Stokes: dashed line, anti-Stokes: solid line. (b) C/A versus the relative delay. The filled and open dots are data sets from two separate measurements (2 minutes averaging time). The average power for the Stokes and anti-Stokes pulses is ~ 100 μW for the filled dots and ~ 50 μW for the open dots. (c) Normalized spectra for the conjugate laser pulses in Fig. 2(b). (d) Phase-matching measurement at the relative delay time -5 ps. The Stokes pump pulse is fixed at the wavelength of 836.3 nm, with its spectrum shown in Fig. 2(c). The anti-Stokes pump is tuned with respect to a central wavelength of 832.7 nm (corresponding to 0 in the wavelength mismatch). Pump condition: Stokes, ~ 100 μW, anti-Stokes, ~ 25 μW. The dots are experimental measurement (10 minutes averaging time). The line is a Gaussian fit.

3. Conclusions

In conclusion, we have proposed and experimentally demonstrated a scheme to generate cross-polarized photon pairs by FWM with cross-polarized laser pulses in a microstructure fiber. These correlated cross-polarized photons can be used to prepare Bell-states for a range of applications. It should be noted that the experiments presented here were implemented with limited pump power and relatively short microstructure fibers. Significant efficiency improvements can be made. Because the number of correlated photons generated in fibers is proportional to $(\gamma PL)^2$ [25, 26], where P is the peak pump power, L is the fiber length, and γ is the nonlinear gain coefficient, a larger γPL product will significantly increase the yield of correlated photons. When group velocity dispersion is not a concern, microstructure fiber of longer length will also help to better resolve the two different overlaps. Longer pulse width with longer overlap times can also help the yield of correlated photons.